POLITECNICO DI TORINO
Repository ISTITUZIONALE

Dynamic performance of a novel tuned vibration absorber with nonlinear friction interfaces

Original
Dynamic performance of a novel tuned vibration absorber with nonlinear friction interfaces / Wang, Yongfeng; Ma, Yanhong; Wang, Hong; Firrone, Christian M.; Hong, Jie. - In: NONLINEAR DYNAMICS. - ISSN 0924-090X. - 112:11(2024), pp. 8831-8848. [10.1007/s11071-024-09347-8]

Availability:
This version is available at: 11583/2989047 since: 2024-05-27T21:58:57Z

Publisher:
SPRINGER

Published
DOI:10.1007/s11071-024-09347-8

Terms of use:

This article is made available under terms and conditions as specified in the corresponding bibliographic description in the repository

Publisher copyright

(Article begins on next page)

26 November 2024

Research Square

Preprints are preliminary reports that have not undergone peer review.
They should not be considered conclusive, used to inform clinical practice,
or referenced by the media as validated information.

Dynamic performance of a novel tuned vibration absorber with nonlinear friction interfaces

Yongfeng Wang (wangyongfeng@buaa.edu.cn)
Beihang University https://orcid.org/0000-0002-3476-6552
Yanhong Ma
Beihang University https://orcid.org/0000-0001-5835-0730
Hong Wang
Beijing Institute of Control Engineering
Christian Maria Firrone
Politecnico di Torino
Jie Hong
Beihang University

Research Article

Keywords: Vibration Suppression , Novel Absorber , Dry Friction , Energy Dissipation

Posted Date: October 12th, 2022

DOI: https://doi.org/10.21203/rs.3.rs-2137697/v1

License: This work is licensed under a Creative Commons Attribution 4.0 International License.
Read Full License

ORIGINAL PAPER

Dynamic performance of a novel tuned vibration absorber with nonlinear friction interfaces

Yongfeng Wang · Yanhong Ma · Hong,Wang · Christian Maria Firrone · Jie Hong

Abstract A novel tuned vibration absorber with frictional interfaces (FTVA) is proposed in this study, combining advantages of the tuned absorber and the nonlinear dry friction damping to dissipate the energy. First, the influence of the mechanism of the nonlinear dry friction damper is introduced using a simplified model with 1-dof tuned mass absorber and the hysteresis friction contact element. Second, a real layout for the FTVA is proposed using a metal strip to tune the vibration absorber, and introducing three frictional contact interfaces with variable normal loads. Both numerical and experimental studies have been carried out which indicate the effectiveness of the novel FTVA. For a well-tuned absorber with properly designed frictional interfaces, the vibration amplitude can be reduced more significantly, and the actual frequency range where vibration amplitudes are limited can be broadened with respect to a classical TVA. The nonlinear contact element contributes to avoid the additional peak vibration generated by the tuned ordinary absorber since the friction damping will be activated as the system response increases to a threshold value. Effects of contact parameters, such as the normal load of the interface, have been deeply investigated as well, which can be optimized to minimize the vibration amplitude. Basic performance of the novel FTVA have been revealed, indicating the potential to suppress vibrations of engineering structures.

Keywords Vibration Suppression · Novel Absorber · Dry Friction · Energy Dissipation

Y. Wang · Y. Ma (✉) · J. Hong
School of Energy and Power Engineering, Beihang University, Beijing, 100191, China
e-mail: mayanhong@buaa.edu.cn

H.Wang
Beijing Institute of Control Engineering, Beijing 100094, China

C.M. Firrone
Department of Mechanical and Aerospace Engineering, Politecnico di Torino, Torino 10139, Italy

1 Introduction

The Tuned Vibration Absorber (TVA) (also known as tuned mass damper (TMD)) is a classical approach to deal with excessive resonance vibrations of structures, and it has been widely used to suppress different vibrations in various fields, such as oscillations of the helicopter rotor [1], rolling motions in ships [2], chatter mitigation for machine tool [3, 4], and seismic responses of buildings under earthquake excitation [5, 6]. The effectiveness of TVA is based on the energy transfer to different regions of the frequency spectrum and the natural frequencies split that are achieved through the tuning of the additional mass. The split of the system natural frequencies shifts the resonance of the primary structure away from the area of interest, resulting in a lower amplitude response at the original frequency region [7].

The typical TVA was first studied by Hermann [8], and the natural frequency is tuned with respect to the concerned frequency range, considering also the counteracted elastic force generated by the stiffness link [9]. Viscous dampers are normally optimized to minimize the peak around the natural frequency [10,11]. A properly designed TVA can optimally suppress the vibration of the primary structure, but improvements are still needed to broaden the effective frequency and globally reduce the response. Plenty of improvements have been carried out, such as multiple inertial elements for different frequency regions [12], or the tuned liquid damper for an improved seismic performance [13], or novel semi-active elements like shape-memory alloys [14], magneto- or electro-rheological fluid [15,16], or even active devices such as piezoelectric actuators [17,18].

For a vibrating mechanical system, the relative motion between contact interfaces is common, which is usually characterized by partial dry friction adhesion leading to hysteresis energy dissipation due to micro-slip. In recent years, friction dampers have been introduced into the tuned vibration absorber (TVA) system, known as FTVA or FTMD [19,20],to improve the performance by the advantage of the nonlinear energy dissipation, besides the direct advantage of

simplifying the construction. In 1990s, Ricciardelli [21] carried out the studies on the SDOF tuned mass damper with linear stiffness and friction damping, and the basic design criteria for the friction TVA systems was presented. Gewei [22] obtained the periodic response of the structure with FTVA under a harmonic base excitation, by using the harmonic balance method, and the effects of the friction coefficient on the structural response were described. Also, Brezeski [23] proved that the proper friction setup can dramatically limit the resonance peak.

A rich scientific literature is available to better understand and model the friction phenomenon caused by alternating motion and the corresponding quantification of energy dissipation and damping introduced in the system. Early studies focused on the stick-slip phenomenon [24] and hysteretic behaviors [25,26] in the case of relatively small vibrations. The hysteresis spring friction element, or Jenkins contact element, consists of a spring in series with a Coulomb friction element, it is often used to model the macro slip behavior of the contact which occurs when the contact status is characterized, during a vibration period, to a local elastic deformation and a full slip of the two surfaces [27]. New types of nonlinear damper-hysteretic friction tuning inertia damper (HFTID) were also proposed [28], which can significantly improve the performance of the TMD for machining chatter suppression [29,30]. Furthermore, Laxalde [31,32] investigated the complex nonlinear modal features of a 2-DOFs system with grounded dry friction, and the simulation results showed that the modal damping was dependent on the modal amplitude. Zhang [33] presented an integrated analytical and experimental study on the vibration absorber with nonlinear frictional interfaces, and the modelling and tuning technique was provided.

Plenty of studies on the tuned vibration absorber have been done in previous studies, which proved that the dry friction may improve the performance in reducing the vibrations. However, the mechanism of the energy transmission and dissipation in FTVA haven't been clearly revealed, though the basic dynamical characteristics have been investigated by simulation or experiments. While most studies are dedicated to model the phenomena using the simplified lumped-spring model, new ideas about absorbers suitable for practical engineering solutions are not common. Thus, the design method of the FTVA for a more complex flexible mechanical system still needs to be developed.

In this paper, a novel tuned vibration absorber with nonlinear friction interfaces is presented and studied. The corrugated metal strip with tuned geometry and mass is chosen to form the absorber, which has been tuned considering the dynamical features of the primary structure. The absorber is purposely designed to introduce the friction interfaces, considering the normal contact load as a tunable parameter which can be adjusted for optimal performance. Both numerical and experimental studies have been carried out, which confirm the effectiveness of the novel absorber for the suppression of vibrations. The effects of the presented device on energy transmission and dissipation indicate the relevant potential in engineering applications.

2 Mechanism Study of the Novel FTVA

In this section, a 2-DOFs model with Frictional Tuned Vibration Absorber (FTVA) is built, to show the effect of friction on the system dynamics. The dynamical response, as well as the energy transfer and dissipation, are investigated and used as the theoretical guideline for the design of the absorber.

2.1 Tuned vibration absorber with friction elements

The system to be investigated in this section is presented in Fig. 1, consisting of a primary or target mass m_1 and a secondary or absorber mass m_2. The primary mass is connected to the ground through a linear spring k_1 and damper c_1, and the primary mass and absorber mass are connected by a linear spring k_2 and damper c_2, while a dry friction element, with hysteretic friction force shown in Fig. 2, is inserted between the two masses. The primary mass is subject to a sinusoidal excitation $q(t)=q_0*\sin\omega t$, leading to the dynamical response of x_1 and x_2, and the relative movement of which is remarked as $y= x_1- x_2$.

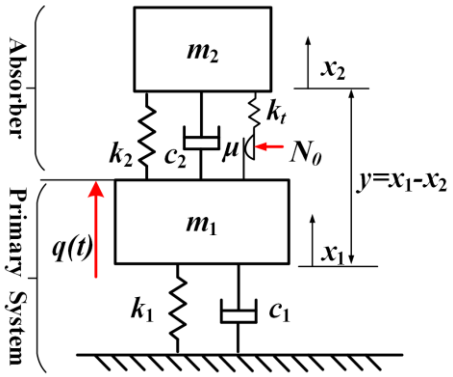

Fig. 1 Illustration of the absorber system with a dry friction element

The widely used Jenkins model is chosen to model the dry friction element, where μ and N_0 are the friction coefficient and normal load respectively, the contact stiffness in tangential direction is k_t. The friction force f_t varies under a periodic excitation load, leading to the hysteresis energy dissipation [34], as shown in Fig. 2. Due to the dry friction element, the system has two

different states, the stick- and slip-state.

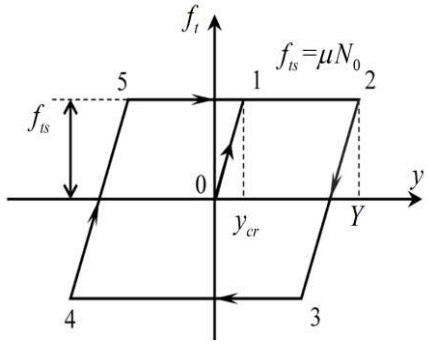

Fig. 2 Illustration of the hysteretic friction force

The tangential friction force f_t depends on the contact state [35]. When the contact interfaces are in stick-state at a low excitation or out of resonance, the relative displacement is relatively small, and the friction force can be expressed as

$$\mathrm{d}f_t / \mathrm{d}y = k_t, \quad |f_t| - \mu N_0 \le 0 \tag{1}$$

The tangential force of the friction element will be enlarged as the relative displacement y increases at a larger excitation force or close to the resonances of the system, until it reaches the critical sliding friction force μN_0. In this case, the system will be in slip-state, and the friction element begins to slide. The friction force at the slip state can be expressed as

$$\mathrm{d}f_t = \mathrm{sgn}(f_t) * (|f_t| - \mu N_0), \quad |f_t| - \mu N_0 > 0 \tag{2}$$

Equation (1) and Equation (2) can be combined to obtain the differential expression of tangential friction force, by deriving which against the time:

$$\begin{cases} \dot{f}_t = (\dot{x}_2 - \dot{x}_1)\,\mathrm{d}f_t / \mathrm{d}y \\ \dot{f}_t = k_t(\dot{x}_2 - \dot{x}_1)H(\mu N_0 - |f|) \\ -\mathrm{sgn}(f_t)H(|f| - \mu N_0)\,(|f| - \mu N_0)/dt \end{cases} \tag{3}$$

$$H(\square) = \begin{cases} 0, (\square) \le 0 \\ 1, (\square) > 0 \end{cases} \tag{4}$$

Where, $\dot{f}_t$ is the first derivative of the tangential friction force against time, while $\dot{x}_1$ and $\dot{x}_2$ represent the first derivative of displacements with respect to time, or the velocity response in other word.

Based on the above formulas, the friction force, relative displacement and relative velocity can be obtained at a specific time instant, by integrating the known velocity and friction force expressed in a differential form.

Based on the expressed friction force f_t, the dynamic equation for the 2-DOFs system with dry friction element, as shown in **Fig. 1**, can be obtained:

$$\begin{cases} m_1\ddot{x}_1 + c_1\dot{x}_1 + k_1x_1 - c_2(\dot{x}_2 - \dot{x}_1) - k_2(x_2 - x_1) \\ + f_t = q(t) \\ m_2\ddot{x}_2 + c_2(\dot{x}_2 - \dot{x}_1) + k_2(x_2 - x_1) - f_t = 0 \end{cases} \tag{5}$$

The system shown in **Fig. 1** is a nonlinear system in nature, with hysteresis friction force at local contact point. Based on the harmonic balance theory in Ref. [36], the nonlinear friction force f_t can be expressed in the form of equivalent stiffness and equivalent damping for simplification, which is

$$f_t(x_1, x_2, \dot{x}_1, \dot{x}_2) \approx \begin{bmatrix} k_{eq} & -k_{eq} \\ -k_{eq} & k_{eq} \end{bmatrix} \begin{Bmatrix} x_1 \\ x_2 \end{Bmatrix} + \begin{bmatrix} c_{eq} & -c_{eq} \\ -c_{eq} & c_{eq} \end{bmatrix} \begin{Bmatrix} \dot{x}_1 \\ \dot{x}_2 \end{Bmatrix} \tag{6}$$

k_{eq} is the equivalent stiffness, and c_{eq} is the equivalent damping, which can be expressed as:

$$k_{eq} = \frac{k_t}{\pi}\left[\cos^{-1}\left(1 - \frac{2\mu N_0}{k_t Y}\right) - \frac{1}{2}\sin\left(2\cos^{-1}\left(1 - \frac{2\mu N_0}{k_t Y}\right)\right)\right] \tag{7}$$

$$c_{eq} = \frac{4\mu N_0 (Y - y_{cr})}{\pi\omega Y^2} \tag{8}$$

Where $Y = |x_1 - x_2|$ is the amplitude of the relative movement y between the primary mass and the absorber, and $y_{cr} = \mu N_0 / k_t$ is the critical value for the sliding displacement.

The parameters used in simulation works are listed in Table 1. The initial amplitude of the excitation force $q(t)$ applied on the primary mass is 10kN, while the initial friction coefficient μ and normal load N_0 for the dry friction element is 5kN, which is variable for the effect on dynamics.

Table 1 Parameters of the model used in simulation

Physical Quantity	Value	Unit
m_1, m_2	10, 0.5	kg
k_1, k_2	1E6, 5E4	N/m
c_1, c_2	0.1, 0.1	
k_t	5E4	N/m
μ	0.5	

2.2 Dynamical characteristics at harmonic excitation

The frequency response function curves (FRFs) of the primary mass, as well as the absorber, are shown in Fig. 3, based on the harmonic balance method and the parameters listed in Table 1. The dynamical response of the system with Frictional Tuned Vibration Absorber (FTVA) are compared with the system without absorber (black-dotted line), and the response of the system with the tuned absorber but without friction

element (red-solid line).

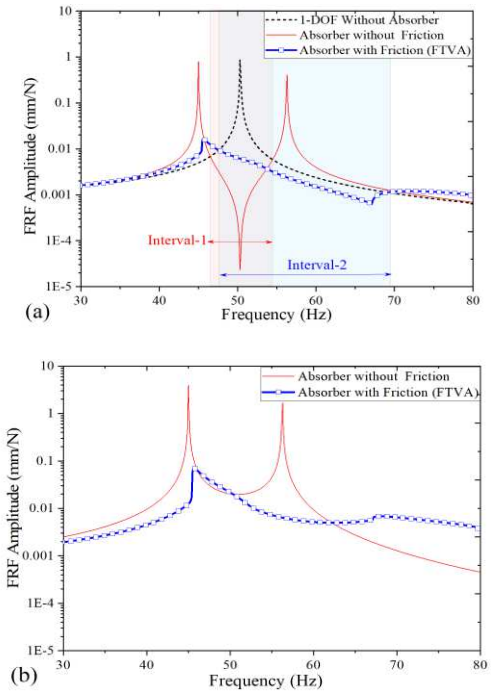

Fig. 3 Frequency responses of (a) the primary mass, and (b) the absorber

The system without absorber (black-dotted line) resonates at about 50.3Hz, causing the vibration response peak. Absorbers can effectively reduce the vibration response at resonance point, by the reaction force derived from the inertia of the absorber mass. Theoretically, the vibration of the well-tuned system can be strongly reduced thanks to the anti-resonance, but it only works at a narrow frequency band closed to the tuned frequency. The vibration amplitude will increase rapidly once the frequency deviates, and there will be additional resonance peak at both sides of the tuned frequency, which can be the same magnitude as the original peak if the damping for energy dissipation is insufficient [37].

The simulation results in Fig. 3 (a) show that, the additional resonance peak can be efficiently eliminated, the maximum reduction close to 98%, as the appropriate dry friction is implemented. Meanwhile, the frequency range for vibration attenuation can also be broadened by over two times for the simulated system. In fact, that of the FTVA system increased from [46.4Hz, 56.3 Hz] to [47.6Hz, 69.3Hz]. Although the amplitude reduction of the system with FTVA is not as remarkable as that with ordinary absorber at the tuned frequency, it is still two orders of magnitude lower than the single resonance of the primary system.

The mechanism for the vibration attenuation of FTVA system can be explained by the special nonlinear lock-up state of the friction element, besides the energy dissipation at the slip-state. When the vibration is low at the frequency lower than the resonance point, the friction element will be in lock-up state, since the breakaway force of the friction element is larger than the induced tangential force. In this state, the relative displacement between absorber and the primary can be ignored, and it can be treated as one larger mass system. Thus, the additional resonance peak caused by the inertia of absorber mass can be eliminated.

The response of the system increases as the excitation frequency gets close to the resonance frequency of the primary system, which will finally break the lock-up state as the breakaway force of the friction element is overcome. Then, the slip-state will be the main feature of the system, and the sliding dry friction is able to dissipate the vibration energy efficiently. The dry friction element can be tuned, so that the breakaway force can be overcome only in a certain frequency range.

The breakaway force of the friction element mainly depends on the friction coefficient μ and the normal load N_0, which will influence the lock-up or slip state under certain excitation force. Fig. 4 shows the frequency responses of the system with FTVA with different normal load N_0.

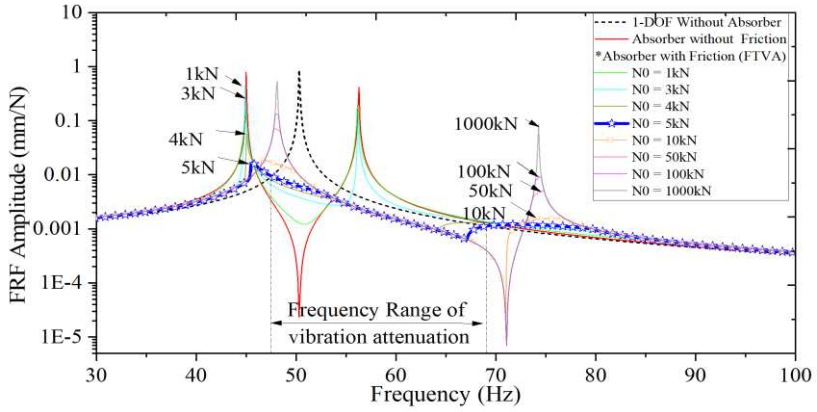

Fig. 4 Frequency responses of the system with FTVA in different normal load N_0

For the friction element in slip-state, the friction force ($f_f=\mu N_0$) depends on the normal load N_0, which has a great influence on the dynamical response of the system. As shown in **Fig. 4**, the lowest response achieved by an optimal normal force (N_0=5kN), which causes ideal alternation between sticking and slipping, in a similar fashion as in Ref. [38]. For the optimal value, the system is in the stick phase up until the point at which the system close to resonance, where the masses inertia in vibration initiate a breakaway, and lead to the energy transmission and dissipation. The vibration decreases at a rate faster than the square of the frequency away from the resonance, such the slip-state is not initiated again after certain frequency point. Since the system is nonlinear, the considered curves are only valid for the considered excitation.

At small normal load, the slip-state will appear at low vibration away from the resonance frequency with a tiny the friction force, which t has very limited influence on the vibration response. Thus, the FTVA acts more like an ordinary absorber, such as the curve when N_0=1kN shown in Fig. 4.

The excessive load may also break the expected condition, which can be described by the example with N_0=1000kN. The friction element is still in stick-state around the resonance point, since the breakaway force is too large to be overcome by the mass's inertia in vibration. Thus, the energy consumption due to the sliding will not appear, and the dynamical response of the system mainly affected by the absorber mass and the tangential contact stiffness of the friction element.

2.3 Energy transmission and dissipation

The energy dissipation rate η_{dis}, expressed by the ratio of dissipated energy and the total input energy of the system as equation (9), is used to assess the absorber efficiency [39]. The amplitude of the system response is time-dependent, and the average energies over period of time by at least an order of magnitude is used [40].

$$\eta_{\text{diss}}=\frac{E_{\text{diss}}}{E_{\text{total}}}\times 100\%=\left(1-\frac{E_{\text{out}}}{E_{\text{total}}}\right)\times 100\% \tag{9}$$

Where E_{total} is the total energy input to the vibration system; E_{diss} is the energy dissipated by the damper; E_{out} represent the energy stored in the system in the form of kinetic energy and potential energy, or that transferred to the other adjacent system.

For the vibration system given in Fig. 1, the dissipated energy E_{diss} not only comes from the linear damper of primary system c_1, or the linear damper of absorber c_2, but also generated by the sliding of the friction element. The energy dissipation at the time period $[t_1,t_2]$ can be expressed as

$$\begin{aligned}E_{\text{diss}}&=W_{\text{primary,linear}}(t)+W_{\text{damper,linear}}(t)+W_{\text{Friction}}(t)\\&=\int_{t_1}^{t_2}c_1\dot{x}_1^2(t)\,\mathrm{d}t+\int_{t_1}^{t_2}c_2\left[\dot{x}_2(t)-\dot{x}_1(t)\right]^2\mathrm{d}t\\&\quad+\int_{t_1}^{t_2}c_{eq}\left[\dot{x}_2(t)-\dot{x}_1(t)\right]^2\mathrm{d}t\end{aligned} \tag{10}$$

Where c_{eq} is the equivalent damping of the friction element, which is given in eq.(7).

The energy E_{out} consists of all the energy stored in the primary system and absorber, mainly in the form of kinetic energy or potential energy, which can be expressed as

$$\begin{aligned}E_{out}&=T_{\text{primary}}(t)+V_{\text{primary}}(t)+T_{\text{damper}}(t)+V_{\text{damper}}(t)\\&=m_1\dot{x}_1^2(t)/2+k_1x_1^2(t)/2+m_2\dot{x}_2^2(t)/2\\&\quad+k_2\left[x_2(t)-x_1(t)\right]^2/2\end{aligned} \tag{11}$$

Where T_{primary} and T_{damper} are the kinetic energy of the primary system and the absorber; V_{primary} and V_{damper} represent the potential energy of the primary system and the absorber.

in order to show the energy dissipation in a complex broadband vibration and avoid the effect of energy input characteristics, the initial vibration energy was applied in the form of a half sine pulse for a limited time interval. The total energy input to the vibration system (E_{total}) is shown in Fig. 5, which is

$$E_{\text{total}}=\int_0^{t_1}F(t)_1*x_1(t)\,\mathrm{d}t \tag{12}$$

The force peak amplitude is 10 kN. The time duration of the pulse force is the half vibration period of the resonance frequency of the primary system, which can be expressed as $t_1=T_n/2=\pi/\omega_n\approx 0.06$s.

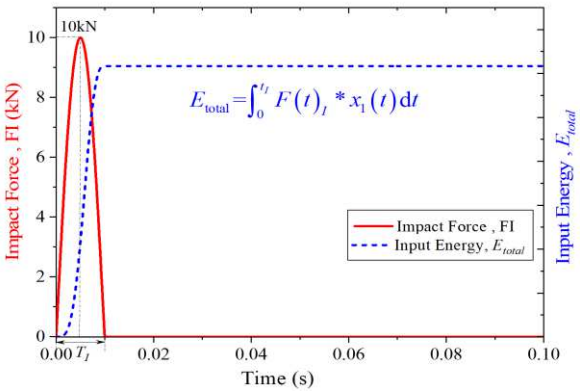

Fig. 5 The excitation and the total energy input

The Newmark method is used to solve the dynamic problem of the system under pulse excitation in time domain, and the responses of the system with or without dry friction elements are shown in Fig. 6. The energy dissipated by different parts is calculated based on equation (10), and the energy dissipation rate (equation (9)) for the system is shown in Fig. 7.

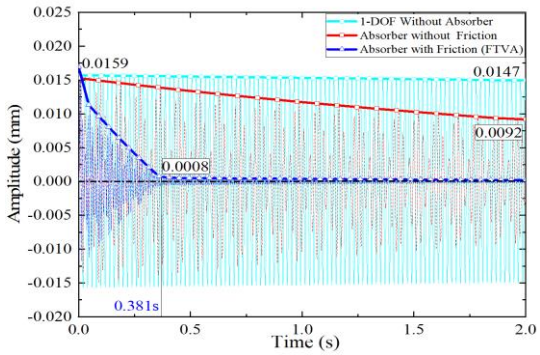

Fig. 6 Vibration amplitude for different system

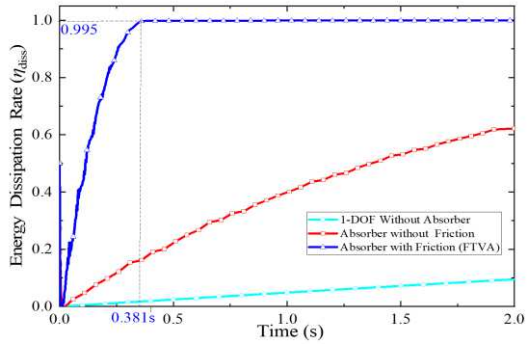

Fig. 7 Energy dissipation rate of the system

For the system without absorber, the vibration energy is mainly dissipated by the linear damping c_1, which is small for most engineer structure, leading to a little energy dissipation rate. Thus, vibration response of 1-DOF system without absorber decreases quite slow, as shown in Fig. 6 and Fig. 7, and the amplitude only decreases by about 5% (0.0157mm to 0.0149mm) in 2 seconds.

The vibration energy input to the primary system can be partly transferred by the absorber, and dissipated by the damping. For the absorber without friction, the transferred energy is dissipated by the linear damping c_2, and the vibration amplitude decreases almost linearly by about 42% in 2s, which is about eight times more than that without damper.

As the dry friction is introduced into the system, over 99% of the input energy can be dissipated in only 0.381s, as the blue curves in Fig. 6 and Fig. 7. The energy dissipation rate is nearly 60 times higher than that of absorber without friction, leading to a faster decrease of the vibration amplitude, which is nonlinear due to the nonlinear stiffness and damping of the friction element. As the amplitude decrease to a small value, the breakaway friction force cannot be overcome, which lead to the stick-state. Then, the energy will be mainly consumed by the linear damping of the system.

Effects of the friction coefficient μ on the energy dissipation is shown in Fig. 8, with a constant normal force (N_0=50kN). Simulation results show that the friction coefficient μ is positively correlated with the energy dissipation, since larger friction force can be acquired in slip-state when μ is larger. But the energy dissipation tends to be steady, as the friction coefficient reaches a threshold value large enough.

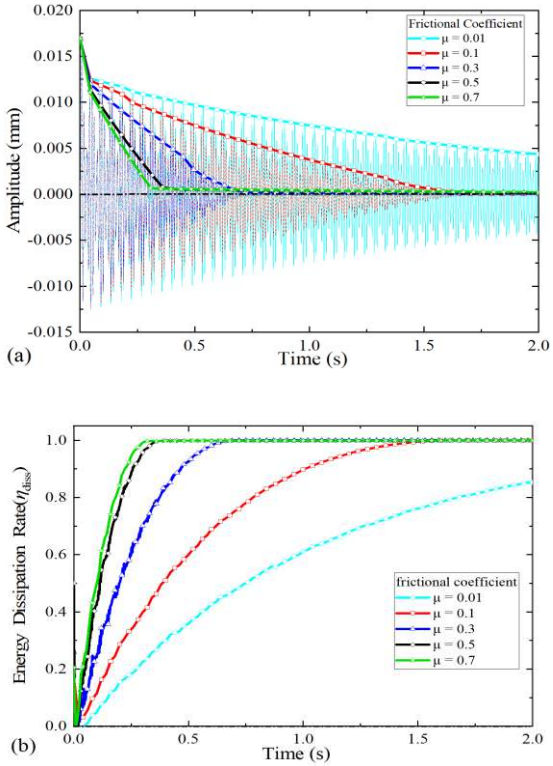

Fig. 8 Influence of the friction coefficient μ on the, (a)vibration amplitude, (b)energy dissipation

The normal load N_0 has a much more complex effect on the energy dissipation, as shown in Fig. 9.

When the normal load is small, N_0 =1N for example, the friction element is mainly in slip-state, and the dynamic response of the system is much like that without friction. Due to the limited friction force at friction interfaces, the energy dissipation is not as fast as that with a larger N_0. The vibration attenuation and the energy dissipation will be accelerated, as the normal load N_0 increases. But it only works in slip-state, when the increased friction force at larger normal load is beneficial to the energy dissipation.

If the normal load is too large, N_0 =500N for example, the lock-up state of the friction element will affect the energy dissipation. The slip-state only exists for a short time under large excitation, as the beginning part of the green curves. The breakaway force can be too large to be overcame as the vibration amplitude decrease, leading to the stick-state with lower energy dissipation. In fact, there is an optimal normal load that lead to the best energy dissipation.

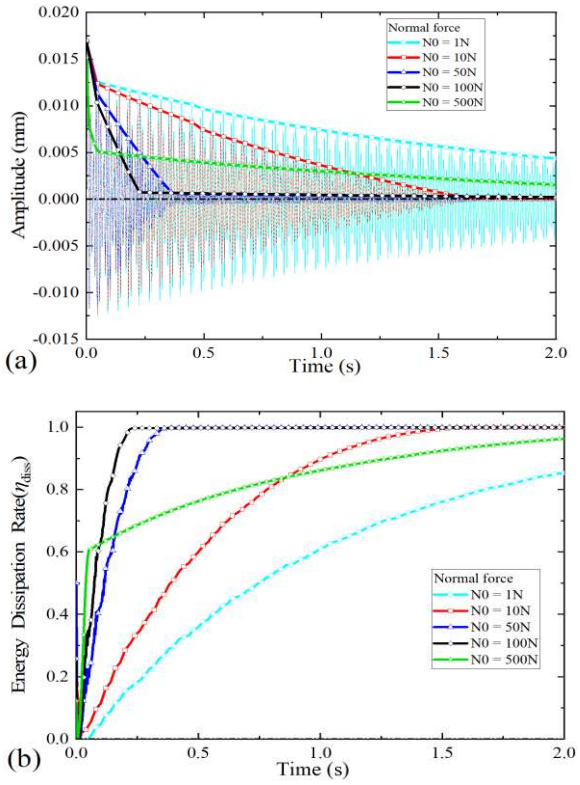

Fig. 9 Influence of the normal load N_0, (a) vibration amplitude, (b)energy dissipation

3 Mechanical Design and Optimization

Mechanical design has been carried out in this section for the novel absorber with friction (FTVA), which can be used in engineering structures. Strategies to form the adjustable friction interfaces was investigated, and the key parameters of the mechanical system were optimized for a better performance.

3.1 Typical features of the novel damper

The proposed novel FTVA is shown in Fig. 10, the natural vibration modes of which can be tuned by the curved sheet with the mass attached at the top end. Contact interfaces are introduced for dry friction using the specially designed support bracket, and the normal contact load can be adjusted through the support bolt.

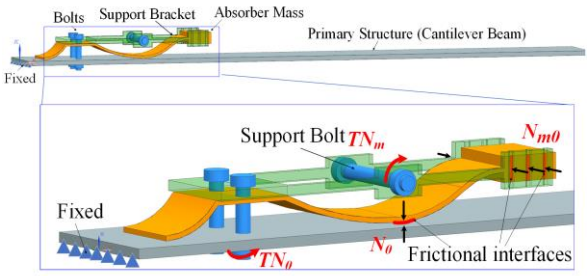

Fig. 10 Diagram of the novel absorber with frictional contact interfaces (FTVA)

The possibility to vary the pre-set values of the contact interfaces helps to tune the dynamical behavior of the metal strip. The primary structure in this study is a cantilever beam (300mm×30mm×2mm), and the typical modes of which are shown in Fig. 11. The curved sheet absorber is tuned, aiming at the 2nd bending of the primary beam, that will lead to the coupling vibration modes. As shown in Fig. 12(a), the absorber vibrates at the tuned frequency, causing the relative motion and friction.

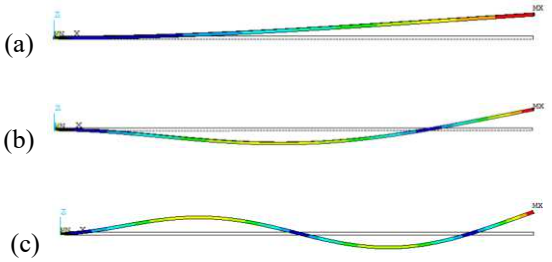

Fig. 11 Typical vibration modes of the primary beam, (a) 1st bending, 16.3Hz, (b)2nd bending, 102.2Hz, (c)3rd bending, 286.4Hz

Besides the curved sheet absorber, the support bracket can also be specially tuned as a friction damper. In fact, the support bracket and the curved sheet can be designed for different vibration modes of the primary cantilever beam, to reduce the vibration in a wider frequency range. The bracket is tuned for the 3rd bending vibration of the beam in this paper, and the coupling vibration is shown in Fig. 12(b).

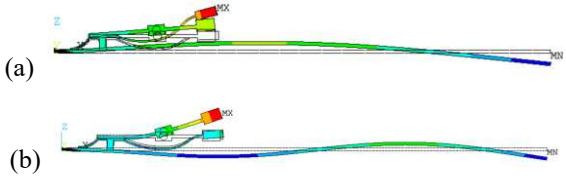

Fig. 12 Coupling vibration modes, (a) 2nd bending of the primary beam and the absorber, (b) 3rd bending of the primary beam and the support bracket

3.2 Methodology for nonlinear responses

The dynamical model with nonlinear contact interfaces is shown in Fig. 13, used for the response of the FTVA system. 20 node brick elements are used to build the finite element model, with a total 33,441 DOFs. The FEA model has uncoupled but conforming (i.e. with nodes at the same geometrical location) meshes at the contact interface, so that node-to-node contact element can be inserted for the nonlinear contact forces. The material properties were chosen according to the standard values for steel: Young's modulus E = 210 GPa, Poisson's ratio ν = 0.33 and density ρ= 7800 kg/m^3.

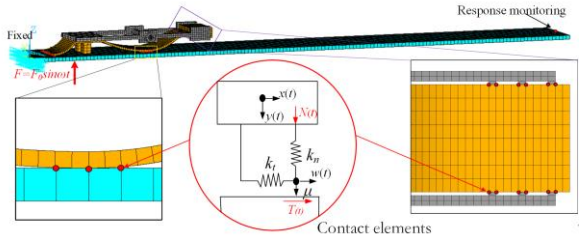

Fig. 13 Dynamic model of the system with FTVA

The governing equations of the dynamic system with friction interfaces can be expressed as:

$$\mathbf{M}\ddot{\mathbf{x}}(t)+\mathbf{C}\dot{\mathbf{x}}(t)+\mathbf{K}\mathbf{x}(t)=\mathbf{F}_{\mathbf{E}}(t)+\mathbf{F}_{\mathbf{NL}}(\mathbf{x},\dot{\mathbf{x}},t) \tag{13}$$

Where the vector $\mathbf{F}_{\mathbf{E}}(t)$ represents the time-varying external forces, and the vector $\mathbf{F}_{\mathbf{NL}}$ is the nonlinear force vector produced at the contact interfaces, consisting of the normal force $N(t)$ and the friction force $T(t)$ in tangential direction.

The widely used node-to-node contact elements were applied at the interface for the contact force, and the application is available in the technical literature about dampers with friction, such as under-platform dampers [41] and the ring dampers [42]. A schematic representation of the contact model is given in Fig. 13, with periodic relative displacements in the tangential $x(t)$ and normal direction $y(t)$. The normal force $N(t)$ depends on the static preload N_0 and the relative normal displacement $y(t)$ by the following relation:

$$N(t)=\max[N_0+k_n y(t),0] \tag{14}$$

Lift-off can occur for a large negative $y(t)$, and no tangential forces are allowed, and a negative N_0 may be used to model an initial separation between coupled nodes.

The tangential contact forces depend on the contact state, which is expressed as:

$$T(t)=\begin{cases} k_t[x(t)-w(t)] & \text{stick state} \\ \mu N(t)\,\mathrm{sgn}(\dot{w}) & \text{slip state} \\ 0 & \text{lift-off state} \end{cases} \tag{15}$$

where $w(t)$ is the amount of slip displacement of the slider at each time, which can be accordingly computed as follow:

$$w(t)=\begin{cases} w(t-\Delta t) & \text{stick state} \\ u(t)-\mu N(t)\,\mathrm{sgn}(T(t))/k_t & \text{slip state} \\ u(t) & \text{lift-off state} \end{cases} \tag{16}$$

where Δt is the time step in the numerical study [43].

Stick, slip, and lift-off may alternate each other during a cycle of oscillation, which will lead to different hysteresis cycles, and an example is shown in Fig. 14 when the relative tangential and normal displacements are in-phase single harmonics. The slip state occurs as the tangential force exceeds the coulomb limit $\mu \cdot N(t)$, and the lift-off state appears if the normal force $N(t)$ is zero.

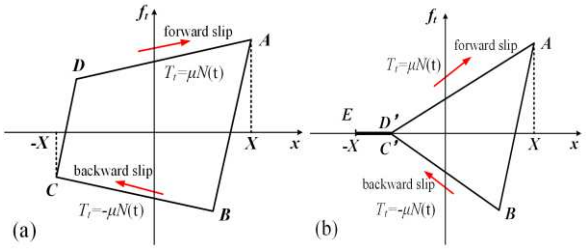

Fig. 14 Typical hysteresis cycles at contact nodes for different states, (a)no lift-off, (b)partial lift-off

The coupling between the normal and tangential directions ensures that the variation can be captured, and the key point is the evaluation of the contact parameters. The parameters used here were based on the data published in Ref. [44], a friction coefficient μ=0.5 is used, and the tangential and normal contacts stiffness are normalized over the contact area $k_t = k_n$ =3×10^4 *N/mm*^{3}. The values of the normal loads (or the gap parameters) are different which were based on the nonlinear static contact analysis (assembly simulation).

The forced responses of the system were numerically calculated following the alternating frequency/time method (AFT) [45], as shown in Fig.15, using a MATLAB in-house developed software. The multi-harmonic balance method (MHBM) was used to calculate the steady-state forced response of the system, while the nonlinear contact forces are computed in the time domain.

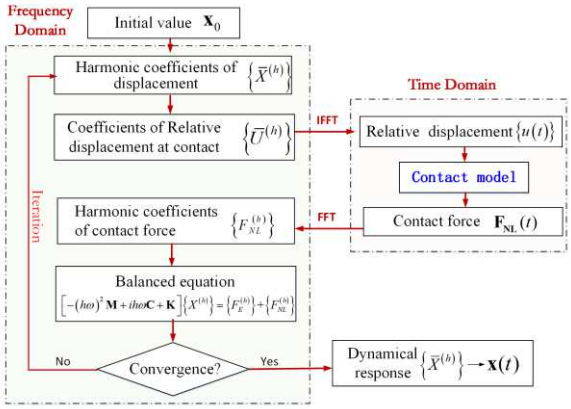

Fig. 15 Flow chart of the forced response calculation

The periodical excitation forces $\mathbf{F}_{\mathbf{E}}$, contact forces $\mathbf{F}_{\mathbf{NL}}$, as well as the nonlinear displacements $\mathbf{x}(t)$ can be approximated with a Fourier series:

$$\begin{cases} \mathbf{x}(t) = X^{(0)} + \Re\left(\sum_{h=1}^{N_H} X^{(h)} e^{ih\omega t}\right) \\ \mathbf{F_E}(t) = F_E^{(0)} + \Re\left(\sum_{h=1}^{N_H} F_E^{(h)} e^{ih\omega t}\right) \\ \mathbf{F_{NL}}(t) = F_{NL}^{(0)} + \Re\left(\sum_{h=1}^{N_H} F_{NL}^{(h)} e^{ih\omega t}\right) \end{cases} \quad (17)$$

where N_H is the number of retained harmonics, ω is the fundamental frequency of the excitation force, and the generic harmonic coefficients $X^{(h)}$, $F_E^{(h)}$, and $F_{NL}^{(h)}$ are complex quantities.

By substituting Eqn.(17), the equation of motion in the frequency domain can be expressed as:

$$\left[-(h\omega)^2 \mathbf{M} + ih\omega\mathbf{C} + \mathbf{K}\right]\left\{X^{(h)}\right\} = \left\{F_E^{(h)}\right\} + \left\{F_{NL}^{(h)}\right\} \quad (18)$$

with h=0, 1, ⋯, N_H. The reduced nonlinear equation of motion can be written in the frequency domain if the reduced matrices and vectors are used instead of the full ones. It must be noticed that, the balance Eqn. (18) are coupled to each other, since the harmonic coefficients $F_{NL}^{(h)}$ of the contact force depends on all the harmonic components of the displacement $X^{(h)}$.

The nonlinear differential equations were solved by the Newton-Raphson Method with finite differences. And the contact forces were obtained in time domain, based on the contact model shown in Fig. 13. Inverse Fast Fourier Transform (IFFT) was used for the periodical relative displacements, based on which the nonlinear contact forces $\mathbf{F_{NL}}(t)$ can be acquired by time domain contact model. At each time step, the computed contact force will be transformed into Fourier coefficients $F_{NL}^{(h)}$ using Fast Fourier Transform (FFT) method. The vector of Fourier coefficients will be assembled in balanced equation for the dynamical responses, and the iteration will continue until the convergence condition is met.

3.3 Simulation results and discussions

Fig. 16 shows the typical frequency responses of the system with FTVA, at the monitoring point marked in Fig. 13. The applied excitation force is 10N, with the same initial normal forces N_0 =25N and friction coefficient μ=0.5 for contact elements.

As the results shown in Fig. 16, the well-tuned FTVA reduce the vibration rapidly around the design frequency. In fact, the peak value of the 2nd order response reduced by nearly 86%, which decreases from 147.3mm/s^2/N to less than 15.5mm/s^2/N, while that at the 3rd order decrease from 399.5 mm/s^2/N to about 41.6 mm/s^2/N.

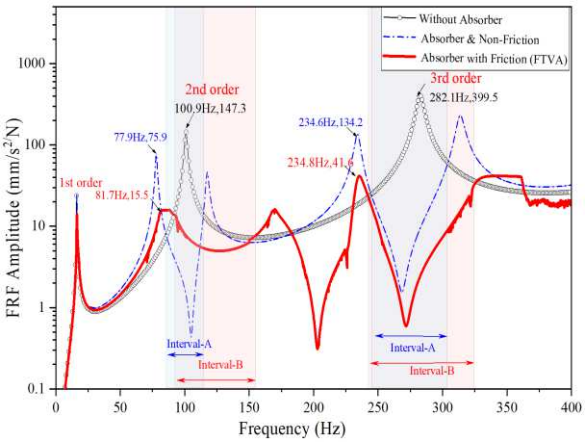

Fig. 16 Typical frequency responses of the system with the tuned absorber FTVA

The friction plays an excellent role in the vibration suppression. For the system using the absorber but without friction (contact elements are deleted in simulation), the vibration only can be reduced at a narrow frequency range (85Hz~115Hz) around tuned frequency, which will increase rapidly once the frequency is deviated. The specially designed frictional contact interfaces not only eliminate the peak response, but also broaden the effective frequency range to [91.6Hz, 155Hz].

Hysteresis curves of tangential force were derived from the contact element, as shown in Fig. 17, to investigate the energy dissipation at frictional interfaces. The results prove that, the contact interface is mainly in stick state at the frequency far from resonance, as shown in Fig. 17(b), since the energy dissipation is slight at a small induced tangential force. But as the responses increase around the resonance frequency, significant hysteresis energy consumption will occur due to the significant friction at larger tangential force, especially for that around tuned frequency of the support bracket aiming at the 3rd order bending mode.

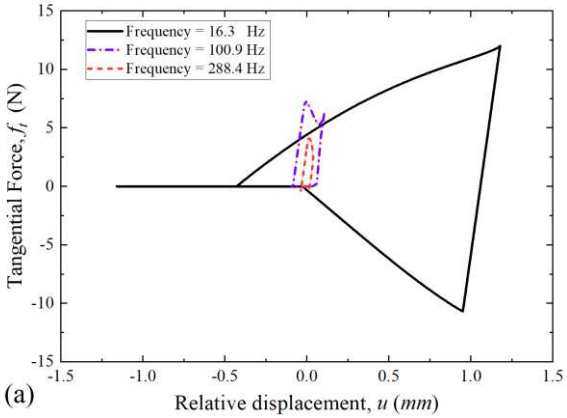

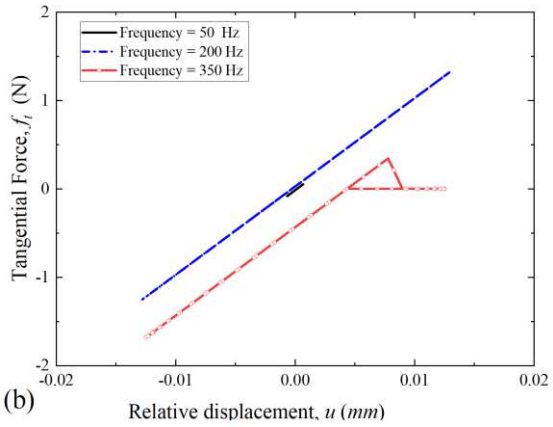

Fig. 17 Hysteresis curves of tangential force versus the relative displacement, (a) around the resonance frequency, (b) far from resonance

Effects of the normal load N_0 are shown in Fig. 18, which are consistent with the results of mechanism studies in section 1. There is an optimal normal pressing force that maximum the energy consumption and minimum the vibration response, while the sliding area and friction force reach the best match.

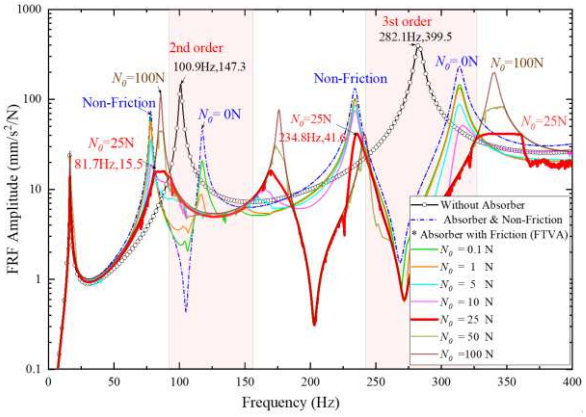

Fig. 18 Effects of the normal load N_0 on the FRFs amplitude of the system with FTVA

A well-chosen normal load N_0 is of vital importance, which may vary for different excitation force. The contact interfaces are always in slip-state, or even lift-off, at small normal force (i.e. N_0=0.1N, the green line in Fig. 18), with a natural frequency similar to that without friction. The amplitude can be reduced by the sliding interfaces, but it's insignificant due to the small energy dissipation under small force. In contrast, the interfaces may always in stick-state under a large normal load (i.e. N_0 =100N), which will change the tuned frequency of absorption and cut down the energy consumption. Above all, for the well-tuned system, it can be in stick phase at low vibration to avoid the additional peak of absorber. While, it can initiate the energy absorption and dissipation under larger vibration force, taking advantages of the inertia of absorber masses.

The dynamical response around 1st resonance is shown in Fig. 19, under varied excitation force. The response can't be reduced by the absorber, since it wasn't tuned for that mode. But the frictional contact interfaces may still dissipate the energy, acting as a damper. The damping induced is influenced by the normal forces, and there is an optimal normal force that maximize the friction energy dissipation for a given excitation condition. When the normal force is small, the damping induced is limited, since the sliding friction force can't be large. On the other hand, if the normal force is so large that can hardly be overcome by the excitation force, the contact interface may remain stick and there may be less energy dissipation.

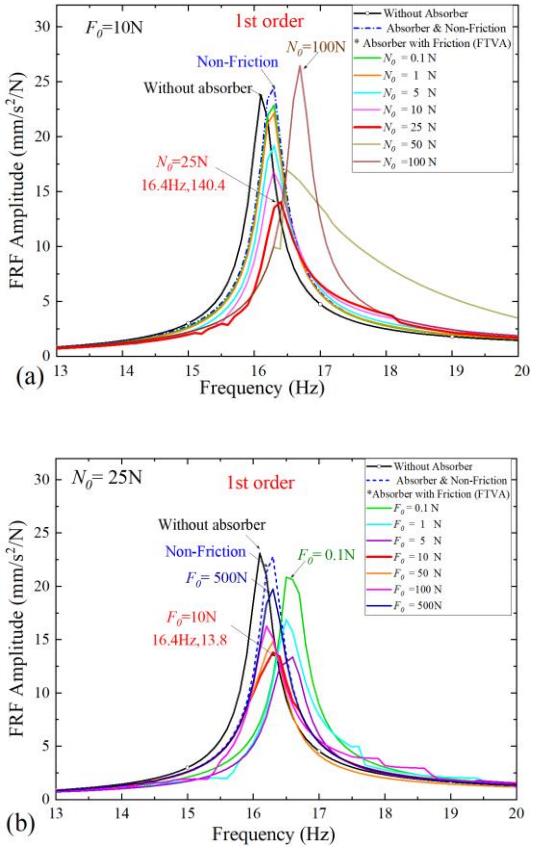

Fig. 19 Dynamical response at the 1st order resonance frequency (untuned), (a)with different normal loads, (b)under different excitation forces

4 Experimental Verification

The novel absorber with friction interfaces shown in Fig. 10 was processed and tested, and the typical results discussed in this section to verify the effectiveness in application.

4.1 Experimental setup

The experimental setup, including the actuator and

sensor, is presented in Fig. 20, which was built based on the working principle in Fig. 10. The cantilever beam used as the primary structure adopts the same size (300mm×30mm×2mm) in simulation, which is mounted at one end on a fixed frame. And the FTVA consists of the curved metal strip absorber and the support bracket, same as that in section 2.

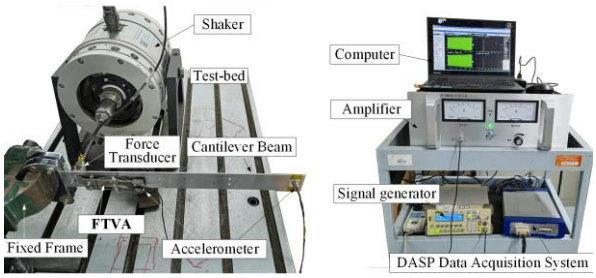

Fig. 20 Experimental system for dynamical testing

The contact status between the curved metal strip absorber and the primary beam are adjusted by the support bolts, as shown in Fig. 21. The curved sheet acts as an ordinary absorber, when the interfaces are separated as shown in Fig. 21(a). While, several frictional contact interfaces can be formed, and the normal force can be adjusted by tightening the bolts, like that in Fig. 21(b).

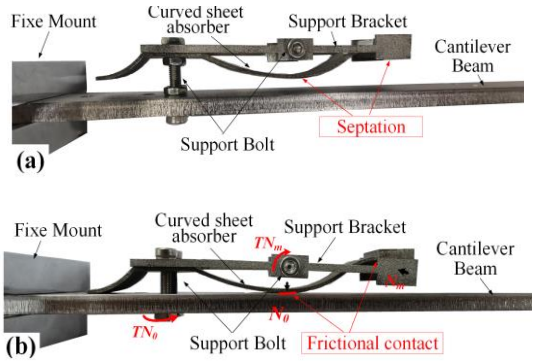

Fig. 21 Absorber in different conditions, (a)septation without friction, (b) frictional contact

As shown in **Fig. 20** and **Fig. 22**, the dynamical excitation was applied by an electromagnetic shaker fixed on the test-bench and is measured by a force transducer, the frequency and magnitude of which are controlled by the signal generator and the amplifier. Vibration responses are tested by the accelerometer glued at the cantilever end of the beam, which are processed by the data acquisition system Coinv DASP 11.0, based on which the frequency response functions (FRFs) are calculated.

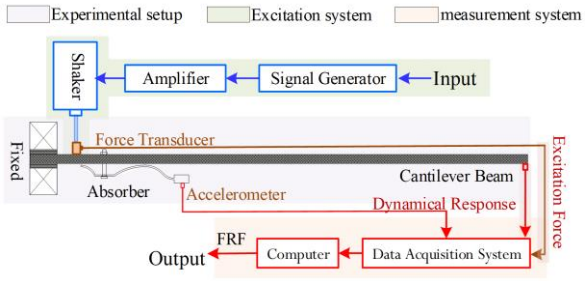

Fig. 22 Schematic view of the experimental system for dynamical response

4.2 Experimental results and discussions

The beam is excited in a frequency range containing the bending vibration mode, and the frequency response are shown in Fig. 23. The experimental results are coincident with simulations, and the relative error is no more than 10% for the calculated resonance frequency, which ensures that the absorber have been well tuned. The error of response amplitude at the higher frequency is much larger, since the vibration is much more sensitive to the miscalculated structural damping.

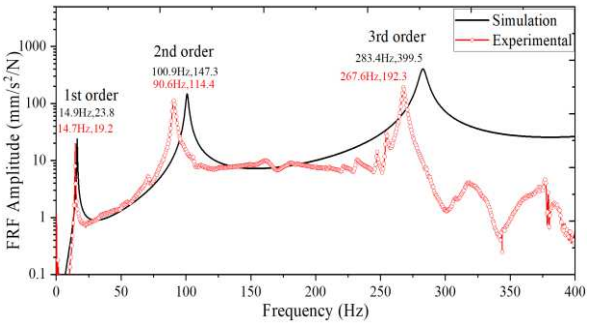

Fig. 23 Comparison of simulation and experimental results at monitoring point

Frequency responses of the system are tested, as shown in Fig. 24, which verify the effectiveness of the FTVA for vibration reduction. The peak amplitudes of the primary beam have been significantly suppressed as the FTVA is applied, though the tested reduction for 2nd order resonance (about 80%) is not as great as the simulated one (about 86%). The reasons for the difference come from both the deviation of processed structure, and the damping from extra interfaces in the frame and test-bed.

The effects of the frictional interface are proved by experimental results as well, by comparing that with or without frictional interfaces. Additional peaks are obvious for the absorber without friction, as the blue curve in Fig. 24, which can be reduced from 74.6 mm/s^2/N to 23.9 mm/s2/N as the frictional interfaces are introduced, decreased by over 68%. The effective frequency range can be broadened as well, and the

vibration can be suppressed at more condition as that discussed in the previous chapter.

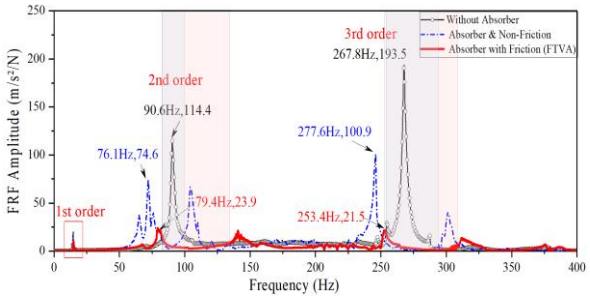

Fig. 24 Testing results of the system with FTVA

Effects of the normal contact load are presented in **Fig. 25**. The normal force between the shaped sheet and the beam was constant with same tightening torque (TN_0=0.15N*m), while the normal loads between the support bracket and the sheet was adjusted by the bolt (TN_m = 0.05~0.3N*m).

For all the tested conditions, the absorber with friction (FTVA) reduce the vibration effectively, and has a better damping effect compared to that without friction. The effects of the normal force (or tightening torque) is similar to the simulation results, though the stick-state or nearly open state under tiny normal force are not easy to be acquired by experiments. There is an optimal normal load that can minimize the vibration amplitude of the system, when the expected energy dissipation can be the best.

For the vibration around the 1st order resonance frequency, the shaped sheet and the support bracket act as a frictional damper, as long as there is relative motion at the contact interfaces. The friction force at the contact interface is larger as the normal force increase, leading to more energy dissipation.

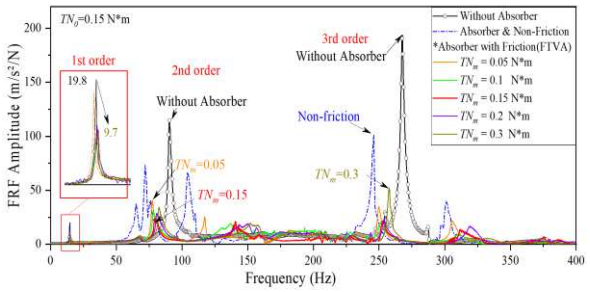

Fig. 25 Influence of the normal contact load on the FRFs amplitude of the system

All in all, experimental results consistent well with the mechanism studies and the simulation results of the novel FTVA, which confirm its effectiveness in vibration suppression. Meanwhile, the effects of the nonlinear friction at contact interface has been proved, and there is an optimal normal force that minimize the response and can maximum the energy dissipation.

5 Conclusions

This paper focuses on a novel tuned vibration absorber with frictional interfaces (FTVA), which combine advantages of the absorber and the friction damper. 2-DOFs system with tuned mass and the hysteresis friction element was proposed, which is used for mechanism study of the system. Based on which, mechanical design and dynamical optimization work for a real layout of the FTVA were carried out, using a developed nonlinear model. Finally, experimental setups were processed and tested, and the effectiveness of the novel absorber was confirmed. Through the experimental and simulation results, following conclusions could be drawn:

1) The nonlinear behavior of the friction creates the special lock-up state, which helps to eliminate the additional resonance peak. The lock-up state is broken under large excitation close to resonance, when the dry friction of the sliding interfaces dissipates the energy efficiently. In fact, the peak value of the response can be reduced by over 80%.

2) The vibration energy input to the primary system can be transferred by the absorber, and dissipated by the damping. The dry friction introduced into the system improved the energy dissipation rate greatly, which can be 60 times better than that of absorber without friction.

The nonlinear friction for vibration suppression depends on the contact parameters of the interface, i.e. the friction coefficient μ and the normal load N_0, which can be optimized to dissipate the energy more efficiently and minimize the vibration amplitude.

3) A real layout for the FTVA is proposed using a metal strip to tune the vibration absorber, and introducing three frictional contact interfaces with variable normal loads. Both numerical and experimental studies have been carried out which indicate the effectiveness of the novel FTVA. The absorber modified by the dry friction not only reduce the vibration amplitude more effectively, but also broaden actual frequency range by over 100%.

4) Experimental investigations of the novel FTVA consistent well with the mechanism and simulation results, which confirm the effectiveness in vibration suppression. Contributions of nonlinear friction at interfaces have been proved, indicating t potential to suppress vibrations of engineering structures.

Acknowledgements: The authors are grateful to the financial support from the National Natural Science Foundation of China (Grant Nos. 52075018 and 52205082), and the Science Center for Gas Turbine Project (Grant Nos. P2021-A-I-002-002).

Data availability All data generated or analyzed during this study are included in this article.

Conflict of interest The authors declare that they have no conflict of interest.

References

[1] Hamouda M N H, Pierce G A. Helicopter vibration suppression using simple pendulum absorbers on the rotor blade[J]. Journal of the American helicopter society, 1984, 29(3): 19-29.

[2] Marcollo H, Gumley J, Sincock P, et al. A New Class of Wave Energy Converter: The Floating Pendulum Dynamic Vibration Absorber[C]//International Conference on Offshore Mechanics and Arctic Engineering. American Society of Mechanical Engineers, 2017, 57786: V010T09A034.

[3] Sims N D. Vibration absorbers for chatter suppression: A new analytical tuning methodology[J]. Journal of Sound and Vibration, 2007, 301(3-5): 592-607.

[4] Habib G, Kerschen G, Stepan G. Chatter mitigation using the nonlinear tuned vibration absorber[J]. International Journal of Non-Linear Mechanics, 2017, 91: 103-112.

[5] Hoang N, Fujino Y, Warnitchai P. Optimal tuned mass damper for seismic applications and practical design formulas[J]. Engineering structures, 2008, 30(3): 707-715.

[6] De Domenico D, Ricciardi G. Earthquake-resilient design of base isolated buildings with TMD at basement: Application to a case study[J]. Soil Dynamics and Earthquake Engineering, 2018, 113: 503-521.

[7] Lupini A, Mitra M, Epureanu B I. Application of Tuned Vibration Absorber Concept to Blisk Ring Dampers: A Nonlinear Study[C]. ASME Turbo Expo 2019: Turbomachinery Technical Conference and Exposition. 2019.

[8] Hermann F. DEVICE FOR DAMPING VIBRATIONS OF BODIES:, US0989958[P]. 1909.

[9] Den Hartog, J.P. Mechanical Vibrations; Courier Corporation: North Chelmsford, MA, USA 1985.

[10] A. Sinha, Vibration of Mechanical Systems, Cambridge, 2010.

[11] Soong T T, Jr B. Supplemental energy dissipation: state-of-the-art and state-of-the-practice[J]. Engineering Structures, 2002, 24(3):243-259.

[12] Srinivasan, A. V. Analysis of parallel damped dynamic vibration absorbers[J]. Journal of Engineering for Industry, 1969, 91(1):282-287.

[13] Novo T, Varum H, Teixeira-Dias F, Rodrigues H, Silva MF, Costa AC, Guerreiro L (2014) Tuned liquid dampers simulation for earthquake response control of buildings. Bull Earthq Eng 12:1007–1024.

[14] Williams K, Chiu G, Bernhard R. Adaptive-passive absorbers using shape-memory alloys[J]. Journal of Sound & Vibration, 2002, 249(5):835-848.

[15] F. Weber, C. Boston, M. Malanka, An adaptive tuned mass damper based on the emulation of positive and negative stiffness with an mr damper, Smart Mater. Struct. 20 (1) (2011) 015012.

[16] F. Weber, Semi-active vibration absorber based on real-time controlled mr damper, Mech. Syst. Signal Process. 46 (2) (2014) 272–288.

[17] L. Kela, P. Vhoja, Recent studies adaptive tuned vibration absorbers/neutralizers, Appl. Mech. Rev. 62 (2009) 0608010608019.

[18] Jalili N, Iv D. Structural vibration control using an active resonator absorber: modeling and control implementation[J]. Smart Materials & Structures, 2004, 13(5):998.

[19] Etedali S, Seifi M, Akbari M (2018) A numerical study on optimal FTMD parameters considering soil-structure interaction effects. Geomech Eng 16:527–538.

[20] Pall AS, Marsh C (1982) Response of friction damped braced frames. J Struct Eng 108:1313–1323

[21] Ricciardelli F, Vickery BJ (1999) Tuned vibration absorbers with dry friction damping. Earthq Eng Struct Dyn 28:707–723.

[22] Gewei Z, Basu B (2011) A study on friction-tuned mass damper: harmonic solution and statistical linearization. J Vib Control 17:721–731.

[23] Brzeski P, Brzeski P, Perlikowski P, Perlikowski P. Effects of play and inerter nonlinearities on the performance of tuned mass damper. Nonlinear Dyn. 2017;88:1027-1041.

[24] Brown, B., Singh, T.: Minimax design of vibration absorbers for linear damped systems. J. Sound Vib. 330(11), 2437–2448 (2010)

[25] Abé M. Tuned mass dampers for structures with bilinear hysteresis[J]. Journal of engineering mechanics, 1996, 122(8): 797-800.

[26] Ricciardelli F, Vickery B J. Tuned vibration absorbers with dry friction damping[J]. Earthquake engineering & structural dynamics, 1999, 28(7): 707-723.

[27] Ferri AA. Friction damping and isolation systems. J Mech des. 1995;117:196-206

[28] Hua X, Tai Y, Huang Z, et al. Optimal design and performance evaluation of a novel hysteretic friction tuned inerter damper for vibration control systems[J]. Structural Control and Health Monitoring, 2021, 28(8): e2775.

[29] Wang M. Feasibility study of nonlinear tuned mass damper for machining chatter suppression. J Sound Vib. 2011;330:1917-1930.

[30] Wang M, Zan T, Yang Y, Fei R. Design and implementation of nonlinear TMD for chatter suppression: An application in turning processes. Int J Mach Tool Manuf. 2010;50:474-479.

[31] Laxalde, D., Salles, L., Blanc, L., Thouverez, F.: Non-linear modal analysis for bladed disks with friction contact interfaces. In: ASME Turbo Expo 2008: Power for Land, Sea and Air, Berlin, Germany, June 9–June 13, p. 457–467 (2008).

[32] Laxalde, D., Thouverez, F.: Complex non-linear modal analysis for mechanical systems: application to turbomachinery bladings with friction interfaces. J. Sound Vib. 322(4), 1009–1025 (2009).

[33] Zhang, X., Xu, J., Ji, J.:Modelling and tuning for a time-delayed vibration absorber with friction. J. Sound Vib. 424, 137–157(2018).

[34] Firrone C M, Zucca S . Modelling friction contacts in structural dynamics and its application to turbine bladed disks[M]. InTech, 2011.

[35] Dayi Zhang, Jianwei Fu, Qicheng Zhang et al. An effective numerical method for calculating nonlinear dynamics of structures with dry friction: application to predict the vibration response of blades with underplatform dampers[J]. Nonlinear Dynamics. 2016: 1-15

[36] Nayfeh A H, Mook A D. Nonlinear Oscillations[M]. Clarendon, 1981.

[37] Dixon J C. The shock absorber handbook[M]. John Wiley & Sons, 2008.
[38] A. Fidlin, M. Lobos, On the limiting of vibration amplitudes by a sequential friction-spring element, J. Sound Vib. 333 (23) (2014) 5970–5979.
[39] Xiong H, Kong X, Yang Z, et al. Response regimes of narrow-band stochastic excited linear oscillator coupled to nonlinear energy sink[J]. Chinese Journal of Aeronautics, 2015, 28(2): 457-468.
[40] Starosvetsky Y, Gendelman O V. Attractors of harmonically forced linear oscillator with attached nonlinear energy sink. II: optimization of a nonlinear vibration absorber[J]. Nonlinear Dynamics, 2008, 51(1): 47-57.
[41] Pesaresi L, Salles L, Jones A, et al. Modelling the nonlinear behaviour of an underplatform damper test rig for turbine applications[J]. Mechanical Systems & Signal Processing, 2017, 85:662-679.
[42] Zucca S, Firrone C M. A METHOD FOR THE DESIGN OF RING DAMPERS FOR GEARS IN AERONAUTICAL APPLICATIONS[C]. Proceedings of the ASME 2010 International Mechanical Engineering Congress & Exposition (IMECE2010). 2010.
[43] Zucca S, Firrone C M. Nonlinear dynamics of mechanical systems with friction contacts: Coupled static and dynamic Multi-Harmonic Balance Method and multiple solutions[J]. Journal of Sound and Vibration, 2014.
[44] Schwingshackl C W, Petrov E P. Modeling of Flange Joints for the Nonlinear Dynamic Analysis of Gas Turbine Engine Casings[J]. Journal of Engineering for Gas Turbines & Power, 2012, 134(12):122504.
[45] Salles L, Blanc L, F Thouverez, et al. Dual Time Stepping Algorithms with the High Order Harmonic Balance Method for Contact Interfaces with Fretting-Wear[J]. Journal of Engineering for Gas Turbines & Power, 2012, 134(3):032503.